MAGNETIC PULSE WELDING OF TUBULAR PARTS - PROCESS MODELING

R. SHOTRI* and A. DE*

*Indian Institute of Technology, Bombay, Mumbai, India (e-mail address –rishabhshotri@gmail.com, amit@iitb.ac.in)

DOI 10.3217/978-3-85125-615-4-41

ABSTRACT

Joining of metallic tubes by fusion welding processes has remained critical due to distortion and dimensional inaccuracy of the joint. Magnetic pulse welding (MPW) facilitates joining of overlapping tubes by controlled plastic deformation under the action of a short electromagnetic impulse without bulk melting of workpiece materials. Thus, MPW can be an efficient recourse for joining of circular sections. However, the short duration and high amplitude electromagnetic forces impose significant challenge to real-time monitoring of MPW. In contrast, computer-based models can provide an opportunity to realize the causative effect of the key process variables on the joint structure and quality quickly and economically. An attempt is therefore presented in this investigation to develop and test a finite element method based numerical model for MPW process with a focus to realize the nature of the magnetic field and electromagnetic forces that facilitates plastic deformation and joining between the flyer and the target tubes. The effect of key process variables is also tested with experimentally measured results reported in independent literature.

Keywords: (Magnetic pulse welding, inductor coil geometry, high strain rate plastic deformation, tube welding)

INTRODUCTION

MPW involves joining of overlapping metallic tubes by the action of an electromagnetic (EM) force, which is generated by applying a high amplitude discharge potential to a shaped inductor coil for a short duration, e.g. a few microseconds. The EM force compels the overlapping region to undergo plastic deformation resulting in a solid state joint with a wavy interface and without any melting. The discharge current, pulse frequency, coil geometry, stand-off distance between the parts and the air gap between the coil and the outer tube, referred to as the flyer tube, influence the rate and extent of plastic deformation, and affect the joint quality.

Although MPW is an established joining process, the complex process mechanism and limited availability of the commercial MPW set-ups have restricted widespread experimental studies. Raoelison et al. [1] studied the effect of discharge voltage and the stand-off distance in MPW of 25 mm diameter aluminium (AA6060T6) tubes. They found the optimum ranges of the discharge voltage and the stand-off distance as 6.5 kV to 7.5 kV, and 1.5 mm to 4.0 mm, respectively. Yu et. al. [2] used MPW to join sheets of dissimilar alloys such as AA1060 and Q235 steel using multi-turn coil. The width of the overlapping region was found as a critical parameter to ensure the joint quality. Faes et al. [3] employed multi-turn coils with field shaper to join thick copper tubes with brass rods. They reported an increase in the EM force on the flyer tube with increase in the overlapping width between the field shaper and the coil. Coil design parameters influence the MPW process significantly and has attracted attention of the researchers. Mishra et al. [4] showed that multi-turn coils with rectangular shaped windings yielded stronger EM force and better joint quality compared to circular shaped windings in MPW of aluminium tubes. Uhlmann et al. [5] used an aluminium field shaper inside a multi-turn copper solenoid coil to augment the EM force.

Although real-time monitoring has helped to understand the causative effect of the operating variables on weld joint structure and quality in several processes, the short duration and high amplitude EM field pose critical challenge to real-time monitoring of MPW. In contrast, computer-based models with coupled electromagnetic and mechanical analyses can provide a better understanding of the evolution of joint interface morphology, structure and property in MPW as function of process variables efficiently. We present here an attempt to simulate MPW through numerical process model based on fundamental relations. In particular, MPW of tubular parts using a solenoid winding coil with field shaper is analysed and tested with corresponding experimentally measured results reported in independent literature.

NUMERICAL INVESTIGATION

MPW of a typical tubular assembly with an axisymmetric multi-turn solenoid inductor coil and a field shaper [Fig. 1] is modelled using finite element method. The two tubes are separated by a standoff distance with an oblique overlapping arrangement as shown in Fig. 1. The outer (flyer) tube and the field shaper are separated by a radial gap that controls the diffusion of the magnetic field. Table 1 provides the ranges of the overlapping width and the radial gap that are considered here. A damped sinusoidal discharge current is considered with peak pulses in the range of 100 kA to 200 kA and pulse frequency in the range of 15 kHz to 25 kHz.

Table 1 Range of processing conditions considered for analysis

Legend	Unit	Value/Range
I (Peak current)	kA	100, 150, 200
f (Pulse frequency)	kHz	15, 20, 25
τ (Damping coefficient)	s^{-1}	1/15000
r (*R*adial gap)	mm	0.8, 1, 1.25, 1.5, 2, 2.5
L (Overlapping width)	mm	10, 13, 15, 18, 20
Flyer tube material	aluminium, copper, titanium, and AISI 1010 steel	
Inner (target) tube material	aluminium and AISI 1010 steel	

NUMERICAL MODELING OF MAGNETIC PULSE PHENOMENON

The damped sinusoidal nature of the current associated with the high amplitude discharge potential in MPW can be expressed as [6]

$$I = I_0 e^{(-t/\tau)} \, sin \, (\omega t) \tag{1}$$

where I_0 is the peak discharge current from the capacitor bank, t is the time of discharge, ω is the frequency (in radians) of the discharge current pulse and τ is the damping coefficient. The resulting EM field can be evaluated following the Maxwell's governing equation as [7,8]

$$\frac{1}{\mu\sigma}\nabla^2 H = \frac{\partial H}{\partial t} \tag{2}$$

where H is the magnetic field intensity, μ is the magnetic permeability and σ is the electrical conductivity. Equation (1) is also referred to as the diffusion equation that further relates the transient magnetic field and the induced eddy current as

$$J = \nabla \times H = \nabla \times (\mu B) = \nabla \times \mu(\nabla \times A) \tag{3}$$

where J is the current density, B is the magnetic flux density and A is the magnetic vector potential. The EM force distribution is further obtained as

$$\mathbf{F} = \mathbf{J} \times \mathbf{B} \tag{4}$$

where **F**, **J** and **B** refer respectively to EM force, current density and magnetic flux vectors. Figure 1 presents the solution domain and the applied boundary conditions for the modelling calculations. The boundary conditions can be listed as follows [9].

- Nil magnetic vector potential (A = 0) over the specified boundary of the solenoid coil,
- Normal component of magnetic flux density vector is continuous along the specified boundary and given as $\mathbf{a_n} .(\mathbf{B_1} - \mathbf{B_2}) = 0$ with $\mathbf{a_n}$ as unit vector normal to the surface.
- Tangential component of magnetic field vector is discontinuous along the specified boundary and expressed as $\mathbf{a_n} \times (\mathbf{B_1} - \mathbf{B_2}) = \mathrm{J_s}$ with $\mathbf{J_s}$ as the surface current density vector.

The transient electromagnetic analysis is undertaken using the commercial finite element software, ANSYS (16) with PLANE233 elements and the magnetic vector potential (Az) as the nodal degree of freedom. The current density (*J*) is applied as an element body load. Table 2 presents the material properties used in the modeling calculations.

Table 2 Material properties considered in modeling calculations

Material	Relative magnetic permeability (μ)	Conductivity (σ), S/m
Copper (Coil windings, field shaper and flyer tube)	0.99	58×10^6
Aluminium (Flyer and target tube)	1.0	38×10^6
Steel (Flyer and target tube)	Estimated from B-H curve [Fig. A1]	2×10^6
Titanium (Flyer tube)	1.0	1.82×10^6
Air (Surrounding region)	1	0

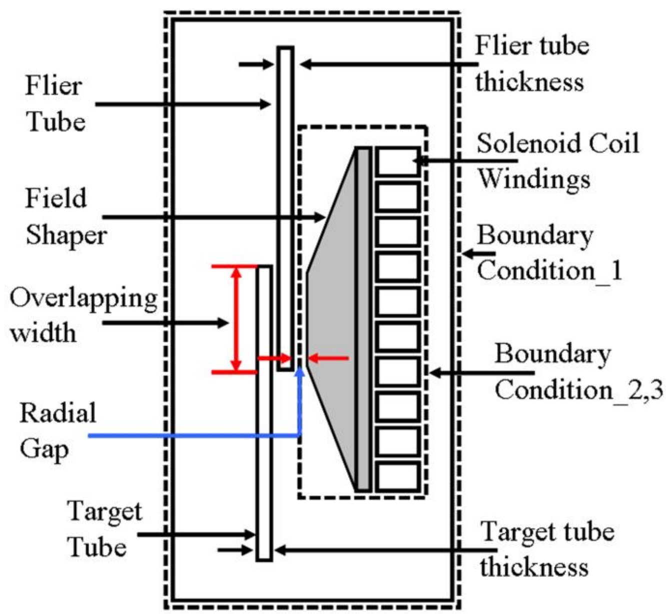

Fig. 1 Schematic assembly of MPW coil with coil design parameters and the boundary conditions.

RESULTS AND DISCUSSIONS

Fig. 2 shows the computed results of magnetic field (B) distribution over an aluminium flyer tube of 1 mm thickness at a time instant of 11 μs for a peak discharge current of 200 kA. The magnetic field is tangential through the radial gap, which in turn induces the eddy current over the flyer tube surface. The concentration of magnetic field vectors increases towards the interacting region of field shaper and the flyer tube surface [Fig. 2 (b)]. The maximum EM force with the aluminium flyer tube was obtained around 68 kN. In contrast, the computed results with a AISI 1010 flyer tube provided the maximum magnetic field and the corresponding EM force as 38 T and 40 kN, respectively with the same processing conditions and the tube dimensions. Thus, the magnetic field and the EM force are influenced both by the flyer tube material and the radial gap parameter. Yu at el. [2] reported a typical EM force of 6.2 kN in MPW of aluminium flyer tube to a steel target tube (~ 1 mm wall thickness) for a peak discharge current of 90 kA and radial gap of 1.2 mm. The smaller EM force computed by these authors is attributed to the lower magnitude of the peak discharge current.

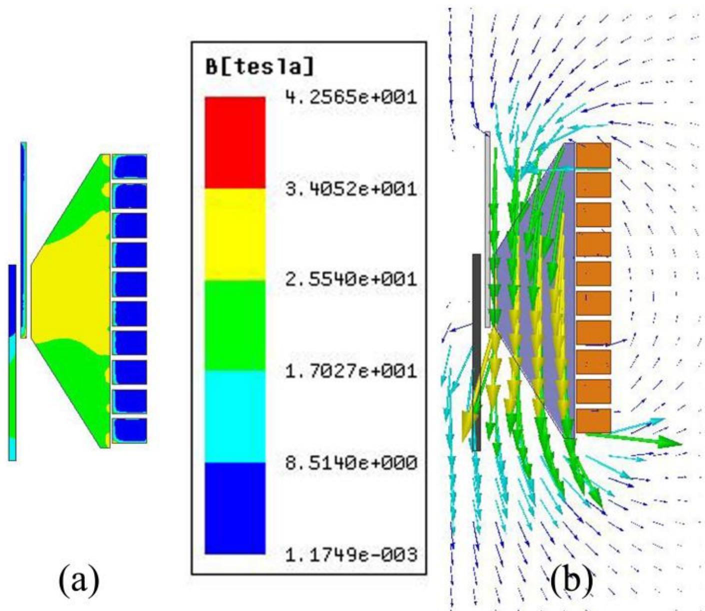

Fig. 2 Computed magnetic field, *B*, at a timeduration of 30 μs: (a) isocontours, (b) vectorial representation. Input conditions: discharge current with a 200 kA peak value, pulse frequency 20 kHz, damping factor 1/15000 s^{-1}, aluminium flyer tube with 1 mm wall thickness and AISI 1010 steel inner target tube with 1.5 mm thickness. Radial gap between flyer and coil is 1 mm.

Fig. 3 shows the computed results of transient current flow and the corresponding EM force in MPW with a aluminium flyer tube for different combinations of peak pulse and its frequency of the discharge current. The current and EM force attain the maximum quickly within the first half cycle of the total duration, and their magnitudes increase with rise in the peak pulse of the applied discharge current [Fig. 3(a, c)]. Increase in pulse frequency of the discharge potential also enhance the peak current and EM force with both reaching faster to the corresponding maximum values as shown in Figs 3(b) and (d). The higher pulse frequency reduces the depth of penetration of the magnetic field into the flyer tube thickness thereby providing more concentration of induced eddy current over the surface and greater EM force. Guglielmetti et al. [10] showed a similar increase in the EM force with increase in the pulse frequency [from 3 kHz to18 kHz] of the discharge potential in MPW of aluminium alloys.

Fig. 4 shows the effect of radial gap on the computed values of the maximum EM force for different combinations of flyer and target tube materials. The maximum EM force over the flyer tube reduces with increase in the radial gap that is attributed to the sparser magnetic field with decreasing intensity at higher radial gaps. For example, the maximum EM force reduces from 72 kN to 64 kN with increase in the radial gap from 0.8 mm to 2.5 mm in MPW of a copper flyer tube with a steel target tube as shown in Fig. 4(a). With all the conditions remaining the same, use of a titanium flyer tube reduces the range of the maximum EM force from 40 kN to 35 kN [Fig. 4(a)] as the electrical conductivity of titanium is much lower compare to that of copper. A comparison of Figs 4(a) and (b) further shows the effect of the target tube material on the EM force for a range of radial gaps. For a radial gap of 0.8 mm and an aluminium flyer tube, the maximum EM force increases from around 67 kN to 71 kN as the target tube material is changed from aluminium to steel [Figs 4(a, b)]. This is attributed to higher magnetic permeability and lower electrical conductivity of steel that has reduced the density of its surface eddy current. As a result, there is lesser interference on the resulting magnetic field over the flyer tube. Shim et al. [11] also reported a decrease in EM pressure from 39 MPa to 16 MPa as the radial gap was increased from 0.76 mm to 6 mm in MPW of 1.5 mm thick aluminium flyer tube with copper target tubes using a single turn solenoid coil.

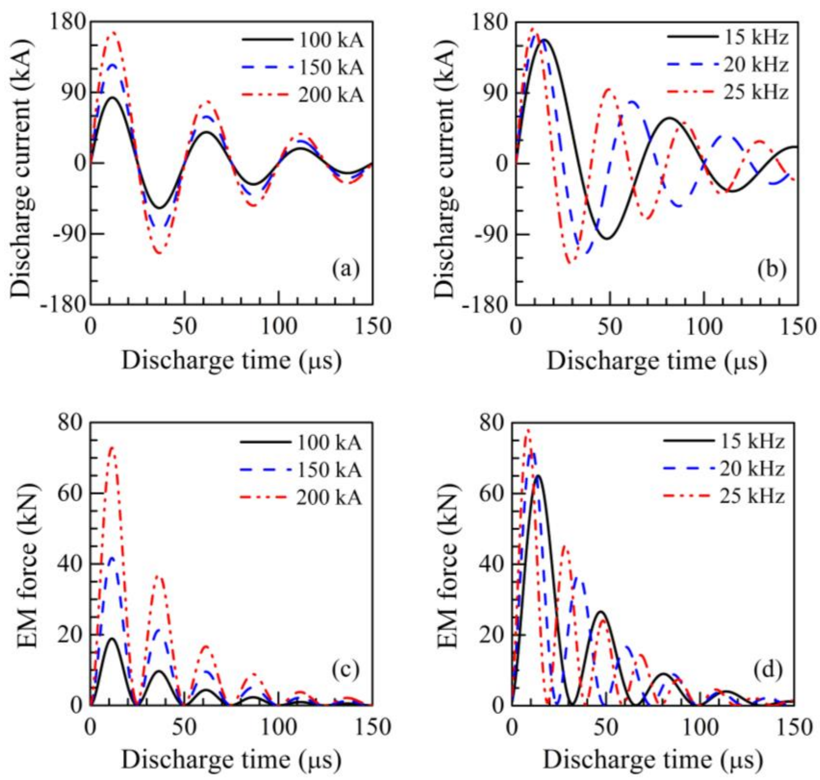

Fig. 3 Influence of peak current and frequency of the damped sinusoidal applied current pulse on the computed magnitude and nature of discharge current and EM forces in MPW with an aluminium flyer tube of wall-thickness 1 mm and radial gap of 1 mm with the coil assembly inside an air region at 150 mm offset along both x- and y- axis respectively.

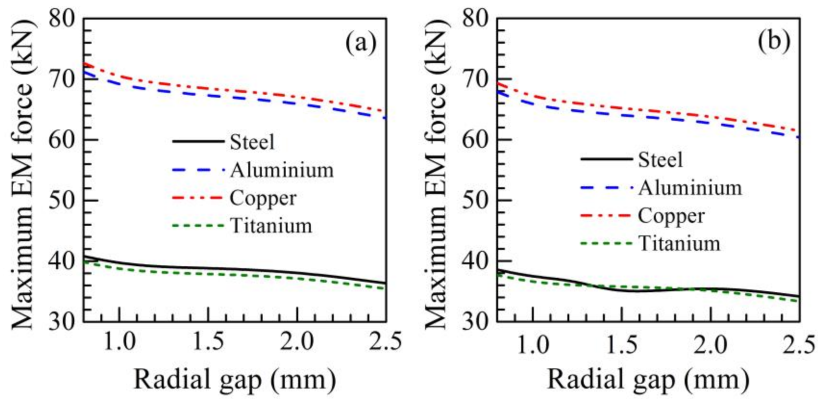

Fig. 4 Effect of radial gap on the computed values of EM force for various combinations of flyer and (a) AISI 1010 steel and (b) aluminium target tube materials. Process conditions considered: discharge potential with a peak current of 200 kA, pulse frequency 20 kHz, time duration 30 μs and damping factor of 1/15000 s^{-1}. The overlapping width and tube thickness were 15 mm and 1.5 mm, respectively.

Fig. 5 shows the effect of overlapping width on the computed values of the maximum EM force for different combinations of flyer and target tube materials. The maximum EM force over the flyer tube decreases with increase in the overlapping width that is attributed to the higher area of EM field distribution. The maximum EM force reduces from around 80 kN to 60 kN with increase in the overlapping width from 10 mm to 20 mm for MPW of an aluminium flyer tube with a steel target tube [Fig. 5(a)]. In contrast, use of a titanium flyer tube reduces the range of maximum EM force from 45 kN to 34 kN that is attributed to lower electrical conductivity of titanium in comparison to aluminium alloys. A comparison of Figs 5(a) and (b) shows the effect of the target tube material on the EM force for a range of overlapping widths. For an overlapping width of 15 mm and a copper flyer tube, the maximum EM force increases from 67 kN to 71 kN as the target tube material is changed from aluminium to steel [Figs 5(a, b)]. This is also attributed to the higher permeability and lower conductivity of steel compared to copper resulting in reduced interference with the magnetic field over the flyer tube when the target tube is of steel. In MPW of aluminium to steel tubes using a single turn solenoid coil, Lorentz et al. [12] observed optimal weld joint condition for overlapping widths of 4 mm to 8 mm. They reported multi-directional and uneven weld propagation for overlapping width higher than half of the width of the coil, although no quantitative analysis based on EM force was provided.

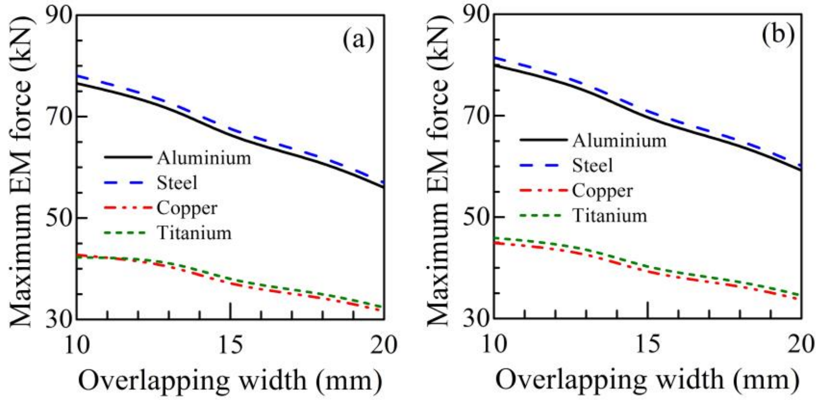

Fig. 5 Effect of overlapping width on the computed values of EM force for various combinations of flyer and (a) aluminium and (b) AISI steel target tube materials. Process conditions considered: discharge potential with a peak current of 200 kA, pulse frequency 20 kHz, time duration 30 μs and damping factor of 1/15000 s^{-1}. The radial gap and tube thickness were 1 mm and 1.5 mm, respectively.

CONCLUSIONS

A numerical model to simulate the underlying transient phenomena in MPW of tubular parts with circular cross-section is developed using finite element method. The model is utilized to examine the effect of key processing variables on the nature and magnitude of magnetic field intensity and EM force for various combinations of flyer and target tube materials that are topical in nature for MPW application. Increase in the radial gap between the coil and the flyer tube was found to result in a sparser magnetic field with reduced magnitude of EM force. In contrast, increase in the overlapping width between the flyer and the target tubes reduces the maximum EM force. Magnetic permeability and electrical conductivity of the tube materials are found to influence the magnetic field intensity and resulting EM force significantly for a given applied discharge potential.

APPENDICES

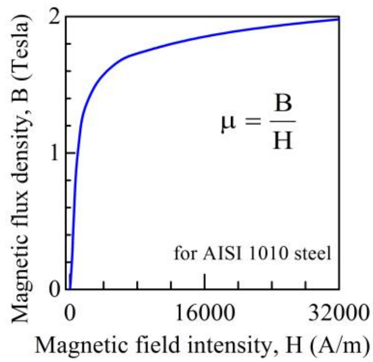

Fig. A.1 Non-linear B-H curve used to assign magnetic permeability of steel.

REFERENCES

1. R. N. RAOELISON, N. BUIRON, M. RACHIK, D. HAYE and G. FRANZ: ‘Efficient welding conditions in magnetic pulse welding’, *Journal of Manufacturing Process* Vol. 14, pp. 372-377, 2012.
2. H. YU and Y. TONG: 'Magnetic pulse welding of aluminium to steel using uniform pressure electromagnetic actuator', *International Journal of Advance Manufacturing Technology*, Vol. 91, pp. 2257 - 2265, 2016.
3. K. FAES, T. BAATEN, W. DE WAELE and N. DEBROUX: ' Joining of copper to brass using magnetic pulse welding', *International Conference of High Speed Forming*, Vol. 4, pp. 84-96, 2010.
4. S. MISHRA, S. K. KUMAR, K. SAGAR, M. MEENA, and A. SHYAM: '40 kJ magnetic pulse welding system for expansion welding of aluminium 6061 tube', *Journal of Materials Processing Technology*, 240, pp. 168-175, 2017.
5. E. UHLMANN, A. ZIEFLE, C. KONIG and L. PRASOL: 'Coupled FEM- simulation of magnetic pulse welding for non-symmetric applications', *International Conference on High Speed Forming*, Vol. 5, pp. 303-314, 2012.
6. M. KIMCHI, H. SHAO, W. CHENG and P. KRISHNASWAMY 'Magnetic pulse welding aluminium tubes to steel bar' *Welding in the World*, Vol. 48, pp. 19-22, 2004.
7. M. V. K. CHARI and S. J. SALON:'Numerical Method in Electromagnetism' *Academic Press*, 2000.
8. M. N. O. SADIKU and S. V. KULKARNI: 'Principle of Electromagnetics', *Oxford University Press*, Vol. 6, 2015.
9. NPTEL: 'Boundary conditions for electromagnetic field', *Electromagnetic Fields nptel.ac.in*, 2009.

10. A. GUIGLIELMETTI, N. BURION, D. MARCEAU, M. RACHIK and C. VOLAT: 'Modelling of tubes magnetic pulse welding', *Conf. on Engineering Systems Design and Analysis*, Vol. 11, pp. 1-12, 2012.
11. J. Y. SHIM, B. Y. KANG, I. S. KIM, M. J. KANG, D. H. PARK and I. J. KIM: ' A study on distributions of electromagnetic force of the dissimilar metal joining in MPW using FEM' *Advance Materials Research*, Vol. 83-86, pp. 214-221, 2009.
12. A. LORENZ , J. LUEG-ALTHOFF, J. BELLMAN, G. GOBEL, C. WEDDLING, E. BEYER and A. E. TEKKAYA : 'Workpiece positioning during magnetic pulse welding of aluminium-steel joints', *Welding Research*, Vol. 95, pp. 101-106, 2016.